Research Article

For reprint orders, please contact: reprints@futuremedicine.com

Personalized Medicine

Zinc finger and interferon-stimulated genes play a vital role in TB-IRIS following HAART in AIDS

Jinmin Ma[‡,1,2,3], Fang Zhao[‡,4], Wei Su[1], Qiongfang Li[1,3], Jiandong Li[1,3], Jingkai Ji[1,3], Yong Deng[4], Yang Zhou[4], Xinfa Wang[4], Huanming Yang[1,5], Nitin K Saksena[1,6], Karsten Kristiansen*[,2], Hui Wang**[,1,7] & Yingxia Liu***[,4]

[1]BGI-Shenzhen, Shenzhen 518083, PR China
[2]Laboratoryof Genomics and Molecular Biomedicine, Department of Biology, University ofCopenhagen, Copenhagen 2100, Denmark
[3]ChinaNational GeneBank, BGI-Shenzhen, Shenzhen 518120, PR China
[4]ShenzhenThird People's Hospital, Shenzhen 518112, PR China
[5]James D. Watson Institute of Genome Science, Hangzhou 310007, PR China
[6]IGO, 19a Boundary Street, Rushcutters Bay, Sydney, NSW, Australia
[7]Department of Engineering Science, University of Oxford,Oxford OX3 7DQ, UK
*Author for correspondence: kk@bio.ku.dk
**Author for correspondence: huiwang789@gmail.com
***Author for correspondence: yingxialiu@hotmail.com
‡Authors contributed equally

Aim: Co-infection in HIV-1 patients with *Mycobacterium tuberculosis* poses considerable risk of developing the immune reconstitution inflammatory syndrome (IRIS), especially upon the initiation of antiretroviral therapy (ART). **Methodology & results:** For transcriptomic analysis, peripheral blood mononuclear cells' whole gene expression was used from three patient groups: HIV$^+$ (H), HIV-TB$^+$ (HT), HIV-TB$^+$ with IRIS (HTI). Pathway enrichment and functional analysis was performed before and after highly active ART. Genes in the interferon-stimulating and ZNF families maintained tight functional interaction and tilted the balance in favor of TB-IRIS. **Discussion & conclusion:** The functional impairment of interaction between *ZNF* genes and interferon-stimulated genes, along with higher expression of *S100A8*/*S100A9* genes possibly forms the genomic basis of TB-IRIS in a subset of HIV patients while on highly active ART.

First draft submitted: 18 Oct 2017; Accepted for publication: 21 Feb 2018; Published online: 09 Jul 2018

Keywords: DEG • HAART • HIV • TB-IRIS • ZNF

AIDS was first diagnosed in 1981, and is caused by HIV [1]. HIV and TB constitute the main burden of infectious disease in poor countries. In the human host, *Mycobacterium tuberculosis* (MTB) and HIV are able to potentiate one another, thereby facilitating the deterioration of immunological functions. Therefore, coinfection in HIV-1 patients with other pathogens (viral and fungal) including MTB poses considerable risk of developing the immune reconstitution inflammatory syndrome (IRIS), especially upon the initiation of antiretroviral therapy (ART). This is usually characterized by clinical progression of a therapeutically treated condition leading to inflammation and other clinical modalities, the hallmark of which is compromised immune system [2]. MTB is one of the most common pathogens associated with IRIS resulting into TB-IRIS [3,4], which is to related fatal co-morbidities.

The proportion of known HIV-positive TB patients on ART was 85% globally [5], and it is noteworthy that more than 30% of those coinfected patients develop the active disease faster than people with HIV infection alone [6]. Currently, the most effective therapy for treating HIV infection is highly active antiretroviral therapy (HAART) [7]. In about 10–32% of AIDS patients, HAART causes severe side effects resulting into IRIS [8].

Although the TB-IRIS was first reported in the early 1990s [9], its overall incidence and underlying mechanisms in immunopathogenesis remain unclear, and appear to be result of unbalanced reconstitution of effector and regulatory T-cells, leading to exuberant inflammatory response in patients who are on HAART. Expansion of TB antigen-specific IFN-γ producing peripheral T-helper cells are generally associated with hyperinflammation in TB-IRIS [10],

but this expansion is not seen in all TB-IRIS cases suggesting that the association might not be the cause [11]. Current studies have mainly focused on the components of the immune system, such as mycobacterial-specific T cells [10,12], but the findings are often confusing and inconsistent between different study populations, especially as in the case of purified protein derivative-specific T cells [10,11]. Contribution of innate immunity to IRIS is well known, along with the presence of inflammatory cells ($CD68^+$ macrophages) [11], enhanced natural killer cell activation and degranulation activity [13,14], increased neutrophil counts in the cerebrospinal fluid [15] of TB-meningitis-IRIS and elevated levels of IL-6 and C-reactive protein in both *Mycobacterium avium*-associated IRIS and paradoxical TB-IRIS [16]. Moreover, the TB-IRIS patients also show elevated expression of pattern recognition receptors such as Toll-like receptor 2 (TLR2) [17]. In monocytes, isolated from HIV-TB coinfected patients, a microarray study has shown evidence of imbalance between the complement effector C1q and the inhibitor C1-INH in those who developed TB-IRIS [18]. Currently, despite a plethora of studies on HIV-TB IRIS, no biomarkers for TB-IRIS have been identified and the underlying genomic basis of HIV-TB-IRIS remains to be elucidated. Furthermore, IRIS has not been delineated at the level of complete human genomes. In this context, and notwithstanding previous research efforts, it is important to iterate that the previous microarray-based studies on macrophages [19] provided limited coverage in comparison to the in-depth coverage with the next-generation sequencing shown in our study. How the next-gene sequencing overcomes the limitations imposed by microarray are discussed by Hurd and Nelson [20].

In this study, through genome-wide study, we have compared TB-IRIS and non-TB-IRIS groups to find genomic modalities that can serve as potential biomarkers for TB-IRIS, along with explaining the underlying mechanisms. Through differentially expressed gene comparisons [21] and pathway enrichment analysis, we have identified key genes related to HIV-TB-IRIS and proposed a hypothetical model to illustrate the possible underlying genomic basis that explains the occurrence of HIV–TB-associated IRIS in coinfected patients. With the development of next-generation sequencing genomic technologies, the genome-wide transcriptome profiling provides holistic approach in gathering genomic information on the status of the immune system, disease development and in visualizing genes involved in these processes [22].

Methods

Sample collection, the peripheral blood mononuclear cell RNA extraction & RNA-seq

All participants were screened for HIV antigens and antibodies via standard ELISA analyses, and these findings were further confirmed by western blotting. $CD4^+$ T-cell counts were obtained by flow cytometry, and the viral loads were measured by real-time quantitative PCR (RT-qPCR). HIV serum-positive patients were also diagnosed for MTB, as assessed by microbiology tests (acid fast bacilli stain, cultures on Lowenstein–Jensen media or GeneXpert PCR), more details are described in Table 1. All clinical tests mentioned above were performed by the Hospital's Clinical Laboratory, which has a certified license issued by the National AIDS Reference Laboratory in PR China Center for Disease Control and Prevention. Treatment for the diagnosed HIV-TB patients consisted of standard fixed-dose chemotherapy for 2 weeks with isoniazid (H), ethambutol (E), rifampicin (R) and pyrazinamide (Z), followed by a combination of HAART and anti-TB treatment (HERZ) [23]. The HAART regimen consisted of Zidovudine plus Lamivudine with Efavirenz, which is the recommended anti-HIV treatment regimen in PR China [24]. None of the patients were treated with HAART before, and there was no evidence of co-infection with hepatitis B or C virus, cytomegalovirus, syphilis, toxoplasma. The criteria for TB-associated IRIS was defined and classified according to the consensus adult TB-IRIS case definition developed by the International Network for Study of HIV-associated IRIS [25]. More details are shown in Table 2.

32 blood samples (5 ml per patient/sample) from 16 participants recruited at the Shenzhen Third People's Hospital from April 2013 to September 2013 were collected. The peripheral blood mononuclear cells (PBMCs) were isolated immediately from the whole blood before, and 2 weeks after the initiation of HAART. The total RNA was extracted from the fresh PBMCs using the Qiagen RNeasy kit (Qiagen, Shanghai, PR China). The mRNAs were purified using oligo(dT) beads then used to construct RNA-seq libraries, which were sequenced on an Illumina HiSeq 2000 sequencing platform (using TruSeqV3 sequencing reagents) at the Beijing Genomics Institute, Shenzhen, PR China (Expected library size: 200 bp; read length: 100 nt and sequencing strategy: paired-end sequencing) as previously described [26].

Table 1. Detailed description of TB and/or TB-immune reconstitution inflammatory syndrome clinical characteristics of HIV-TB-co-infected patients pre- and post-antiretroviral therapy.

Patient	Type of TB	Radiological	Pleural effusion	IGRA	Sputum/BALF test			Time to IRIS occurrence after ART (days)	IRIS duration (days)	New clinical events					
					Smear	*Culture*	*GeneXpert*			*Fever*	*Worsening respiratory symptoms*	*Worsening radiological*	*New/enlarging lymph nodes*	*Other opportunistic infection*	*Drug adverse reaction*
HTI_0	PTB	+	−	+	−	+	+	14	7	+	+	+	−	−	−
HTI_1	PTB	+	−	−	+	+	+	15	12	+	−	+	+	−	−
HTI_2	PTB	+	+	−	−	+	+	13	14	+	+	+	−	−	−
HTI_3	PTB	+	−	−	+	+	+	16	10	+	+	+	+	−	−
HTI_4	PTB	+	−	−	+	+	+	14	11	+	+	+	−	−	−
HTI_5	EPTB (LN)	+	−	−	+[†]	+[†]	+[†]	15	18	+	−	−	+	−	−
HT_0	PTB	+	−	+	+	+	+	NA	NA	−	−	−	−	−	−
HT_1	PTB	+	−	−	−	+	+	NA	NA	−	−	−	−	−	−
HT_2	PTB	+	−	+	−	+	+	NA	NA	−	−	−	−	−	−
HT_3	PTB	+	−	+	+	+	+	NA	NA	−	−	−	−	−	−
HT_4	PTB	+	−	+	+	+	+	NA	NA	−	−	−	−	−	−
HT_5	DTB	+	+	−	−	+	+	NA	NA	−	−	−	−	−	−

+: Positive; −: Negative.

[†]Samples from lymph node aspirate.

ART: Antiretroviral therapy; BALF: Bronchoalveolar lavage fluid; DTB: Disseminated tuberculosis; EPTB: Extra pulmonary tuberculosis; ; HT: HIV-TB^{+}; HTI: HIV-TB^{+} with IRIS; IGRA: Interferon gamma release assay; IRIS: Immune reconstitution inflammatory syndrome; LN: Lymph node; NA: Not applicable; PTB: Pulmonary tuberculosis.

Table 2. Diagnosis of paradoxical TB related immune reconstitution inflammatory syndrome.

Patient	(A) Antecedent requirements			(B) Clinical criteria		(C) Alternative explanations	
	Diagnosis of TB	*TB treatment before ART (weeks)*	*Response to TB treatment*	*Major*	*Minor*	*Other opportunistic infection*	*Drug adverse reaction*
HTI_0	Definitive	2	+	Worsening radiological	Fever and worsening respiratory symptoms	–	–
HTI_1	Definitive	2	+	Worsening radiological and enlarging lymph nodes	Fever	–	–
HTI_2	Definitive	2	+	Worsening radiological	Fever and worsening respiratory symptoms	–	–
HTI_3	Definitive	2	+	Worsening radiological and enlarging lymph nodes	Fever and worsening respiratory symptoms	–	–
HTI_4	Definitive	2	+	Worsening radiological	Fever and worsening respiratory symptoms	–	–
HTI_5	Definitive	2	+	New and enlarging lymph nodes	Fever	–	–

According to consensus case definition published in 2008 [25].
ART: Antiretroviral therapy; HTI: HIV-TB$^+$ with IRIS; IRIS: Immune reconstitution inflammatory syndrome.

Table 3. Patient groups and changes in the number of CD4$^+$ T cells and HIV plasma RNA load before and after highly active antiretroviral therapy treatment.

Group	CD4 (cells/μl)		HIV RNA load (copies/ml)	
	Before HAART	HAART 2 weeks later	Before HAART	HAART 2 weeks later
TB-IRIS (HTI)	$62.5 \pm 46.4^{\dagger}$	190.3 ± 127.3	$3.86 \pm 3.6 \times 10^{6\dagger}$	$2.78 \pm 5.14 \times 10^{4}$
TB-non-IRIS (HT)	249 ± 120.3	330 ± 134.8	$6.76 \pm 11.1 \times 10^{6}$	500 ± 0
HIV-non-IRIS (H)	235 ± 117.6	334.5 ± 111.5	$1.97 \pm 1.74 \times 10^{5}$	500 ± 0

†Before HAART, the CD4$^+$ T-cell count was lower in the HTI group (HTI vs [HT + H], p-value = 0.010, Wilcoxon Rank Sum Test), the HIV-RNA load was higher (HTI vs [HT + H], p-value = 0.023, Wilcoxon Rank Sum Test) in HTI group.
H: HIV$^+$; HAART: Highly active antiretroviral therapy; HT: HIV-TB$^+$; HTI: HIV-TB$^+$ with IRIS; IRIS: Immune reconstitution inflammatory syndrome.

Table 4. Functional domain enrichment using targetmine.

Protein domain	p-value	ZNF genes rate (%)	Interpro ID
Zinc finger C_2H_2-type/integrase DNA-binding domain	3.08×10^{-11}	91.84	IPR013087
Zinc finger, C_2H_2	2.08×10^{-10}	88.24	IPR007087
Zinc finger, C_2H_2-like	2.77×10^{-10}	88.46	IPR015880
Krueppel-associated box	7.96×10^{-10}	97.06	IPR001909

Results depicting the functional domain enrichment of 392 DE genes. The p-value was calculated using the hypergeometric distribution and correction by the Holm-Bonferroni (H-B) method.

Analysis pipeline

Genome-wide transcriptome data from the PBMCs from four HIV$^+$ patients, six HIV$^+$/TB$^+$ patients and six HIV$^+$/TB$^+$/IRIS patients before and after HAART (four H, six HT and six HTI, Table 3) were analyzed using Illumina Hiseq 2000. 32 pair-ends RNA-seq data were produced, with the data volume up to 185 GB.

Pairwise comparisons were carried out for before and after HAART time points for: HT group, HTI group and HT and HTI groups, respectively (Supplementary Figure 4). Differentially expressed genes (DEGs) with

p-value < 0.05, q-value < 0.05 and |Log2 (fold change) | > 1 were identified for each comparison. DEGs in different groups were then uploaded to an online website TargetMine [27] for the pathway analysis. The results were then used for association analysis, and other downstream analyses (Supplementary Figure 4).

Analysis of DEGs

The recommended pipeline of Cufflinks version 2.2.1 [21] was used, with the default parameters set. If six biological replicates are used, the empirical true positive rate of Cuffdiff2 could reach over 85% by adjusting the parameters set, but the empirical false-positive rate still existed [28]. Considering this, Kruskal–Wallis (K–W) significance test among three groups was used in filtering out the false-positive rate. All the values for gene expression were exported as Fragments per kilobase million (FPKM); Reference genome and gene transfer files (GTFs) were from iGenomes UCSC *hg19* gene annotation. Sequence alignments were conducted by using TopHat version 2.0.14 [29].

The DEGs were selected from three groups: HIV-TB group and HIV-TB-IRIS group at pre- and post-HAART stages; HIV-TB group before and after HAART initiation; HIV-TB-IRIS group before and after HAART. No DE genes were detected in analysis of HIV group before and after HAART. The software Cuffdiff2 integrated in the Cufflinks packages was used to find DEGs, with a threshold value (p-value < 0.05, q-value < 0.05 and |Log2 (Fold-change) > 1|) set. Considering the additional influence of TB infection, the FPKM values were extracted from the DEGs selected in group-1). With the FPKM values of HIV group added in, K–W significance test was conducted among three groups. The threshold values were set as p-value < 0.01, FDR (false discovery rate) < 0.05. The selected genes were then used for pathway analysis.

Enrichment analysis

Enrichment analysis was performed using online website TargetMine [27]. TargetMine pathway analysis compiled KEGG pathway and Reactome database as sources. The p-values were calculated by the statistical tools embedded in the online platforms used for analysis herein [27]. The results were filtered by a cutoff adjusted p-value of 0.05 and in order to select functionally significant candidate pathways.

Gene set enrichment analysis (GSEA) was conducted by GSEA [30] with Reactome v5.0 as database. The gene set was set as the method to permute parameters set as default. Nominal p-value < 0.01 and FDR < 0.05 were used as standard filters.

Correlation analysis

Correlation analysis was performed among the enriched genes and HIV load (before and after HAART) by using Spearman Correlation Coefficient in HIV, HIV-TB, HIV-TB-IRIS groups. The results were used for showing whether the enriched genes were significantly correlated with the biological processes and for further explaining the underlying mechanisms.

RT-qPCR validation

Before RT-qPCR, primers were designed using the online tools Primer-BLAST [31] in NCBI (National Center for Biotechnology Information: www.ncbi.nlm.nih.gov/). We selected eight highly expressed genes (genes and the corresponding primers used are listed in Supplementary Table 12) in our candidate DEG sets. A reference gene, *β-Actin* was used in quantifying the gene expression levels. In addition, we selected three, six and one genes from the HTI, HT and H groups, respectively, as templates for the RT-qPCR. Reverse transcription of the candidate RNA sample was performed using the 1st strand cDNA Synthesis kit (Takara). Expression levels were measured with the Step One Plus instrument, according to the standard protocol recommended by the manufacturer (Applied Biosystems, Shanghai, PR China). The relative expression levels of PBMC RNA among the three groups were calculated by the $2^{-\Delta Ct}$ method normalized by *β-Actin* gene.

Results

Clinical comparisons & RNA-seq

Up until now, there is no gold standard for the diagnosis of IRIS, which is mainly based on clinical indices, such as base line $CD4^+$ T-cell counts (<100/μl), deterioration of the condition after the initiation of HAART, and the degree of plasma viremia [4]. In the clinical samples collected, we found that before the initiation of HAART the $CD4^+$ T-cell counts were lower (group HTI vs [HT + H], p-value = 0.010, Wilcoxon Rank Sum Test, Wilcox.test in software R package, with the alternative = less, paired = FALSE), coinciding with higher HIV RNA load (group

HTI vs [HT + H], p-value = 0.023, Wilcoxon Rank Sum Test, Wilcox.test in software R package, with the alternative = less, paired = FALSE) in the IRIS group than that in non-IRIS groups (Table 3). Following HAART in the HTI group, the $CD4^+$ T-cell counts presented a certain degree of comeback concomitant with only slightly decreased HIV-RNA load (Table 3), and with different changes in different groups, implying that there possibly exists an essential biological and genomic distinction between H, HT and HTI groups. Although there were some intragroup differences, more intergroup differences were apparent.

In all 32 samples (16 subjects were studied at pre- and 2 weeks post-HAART time points, four with HIV only, six with HIV and TB without IRIS, and six with HIV and TB who developed IRIS), the RNA-seq data derived from the three groups were mapped to human reference genome, with the average base read of 29 million. The average mapping rate of all samples was 92.52%, whereas the average mapping rates (Supplementary Table 1) of each group were 92.23% (HTI), 92.61% (H) and 92.81% (HT), respectively. Principal component analysis (PCA) was performed on all samples and FPKM values were assessed for each sample before HAART, which distinguished HTI group from the other two groups on PC1 (Figure 1A & B). While the HTI group completely and independently segregated toward the right before HAART from the H and HT groups (Figure 1A), further suggesting the possibility of special biological and gene traits unique to HTI group as discussed before.

Interestingly, following HAART the HT and H groups appeared to show some overlaps with the HTI group (Figure 1B), suggesting that some changes were common, along with some specific differences in the HTI group in comparison to other two groups analyzed pre- and post-HAART in this study. Furthermore, the multigroup PCA analysis combining all pre- and post-HAART samples for the three groups confirmed the distinctness of the HTI group both before and after HAART, with limited crossover in relationship between HTI and HT groups following HAART. This PC analysis also implies the genetic stability of the groups, which is highly critical in making functional assumptions and clinical correlations (Supplementary Figure 1A).

To address these observations of the PCA (Figure 1B), we examined the nature of overlapping DEGs between groups before HAART (Figure 1E), and after HAART (Figure 1F). There were 45 genes that overlapped between three groups after HAART (Figure 1F), 13 of which also overlapped before HAART (Figure 1E) and 32 following HAART between the three groups. Following HAART, the nature of the overlapping genes changed, and most genes (17 of 32 genes – 53%) were focused in functions associated with cell integrity, chromatin, spindle formation, cell proliferation, nucleolar, kinetochore, DNA replication/metabolism and checkpoint functions, G-coupled receptors, microtubule and cell integrins, and so on, which are in sharp contrast with the overlapping genes before HAART that varied considerably in functional annotation, with only some associating with cellular integrity (Supplementary Table 2).

Significant differential expression of ZNF genes in different groups before HAART

For the comparison HT versus the HTI group (intergroup), before HAART, 947 DEGs were identified using Cuffdiff2 tools of Cufflinks packages v2.2.1 with FPKM value normalization and the average value of a gene for each sample was plotted (Supplementary Figures 1B & 4). Following HAART, the total DEGs were 451 between the HTI and HT groups (Supplementary Figure 1C). For distinguishing nonspecific DEGs from the specific ones, and also considering that TB infection was an extra factor that requires stringent DEGs selection, the FPKM values of the H group (before HAART) added in for K–W one-way significance test (with p-value < 0.01, FDR < 0.05) was performed for HTI, HT, H groups together, in order to better understand the TB's influence on gene expression. There were 392 DEGs (197 up-regulated, 195 down-regulated, Figure 1C), which were DEGs among HTI, HT, H groups that were used for pathway analysis (Supplementary Table 3). Similarly compared for intragroup, 88 DEGs were identified after HAART and were analyzed in a similar manner (Figure 1D, Supplementary Figure 4 & Supplementary Table 8).

Pathway analysis between HTI and HT groups was carried out using TargetMine [27] and in this analysis 38 of 392 DEGs were enriched in a significant pathway: the Generic Transcription Pathway (p-value = 1.11×10^{-6}; Supplementary Tables 3 & 4). Among the 38 genes, 30 (79%) of them were the zinc finger protein-coding genes. Comparing the FPKM values in HTI, HT and H groups, respectively, for the ZNF genes, we found that the expression level of 30 ZNF genes was considerably lower in the HTI group (p-value < 0.01, FDR < 0.05, K–W test, Figure 2A) in comparison to the HT group. Following the qPCR analysis, we validated the consistent expression trend of the ZNF genes (*ZNF264, ZNF41, ZNF441*) in the three groups, which was agreement with the analysis of the FPKM values shown in Supplementary Figure 2. While we also noticed that after HAART, ZNF genes described above did not show significant difference from that before HAART in the HTI or HT

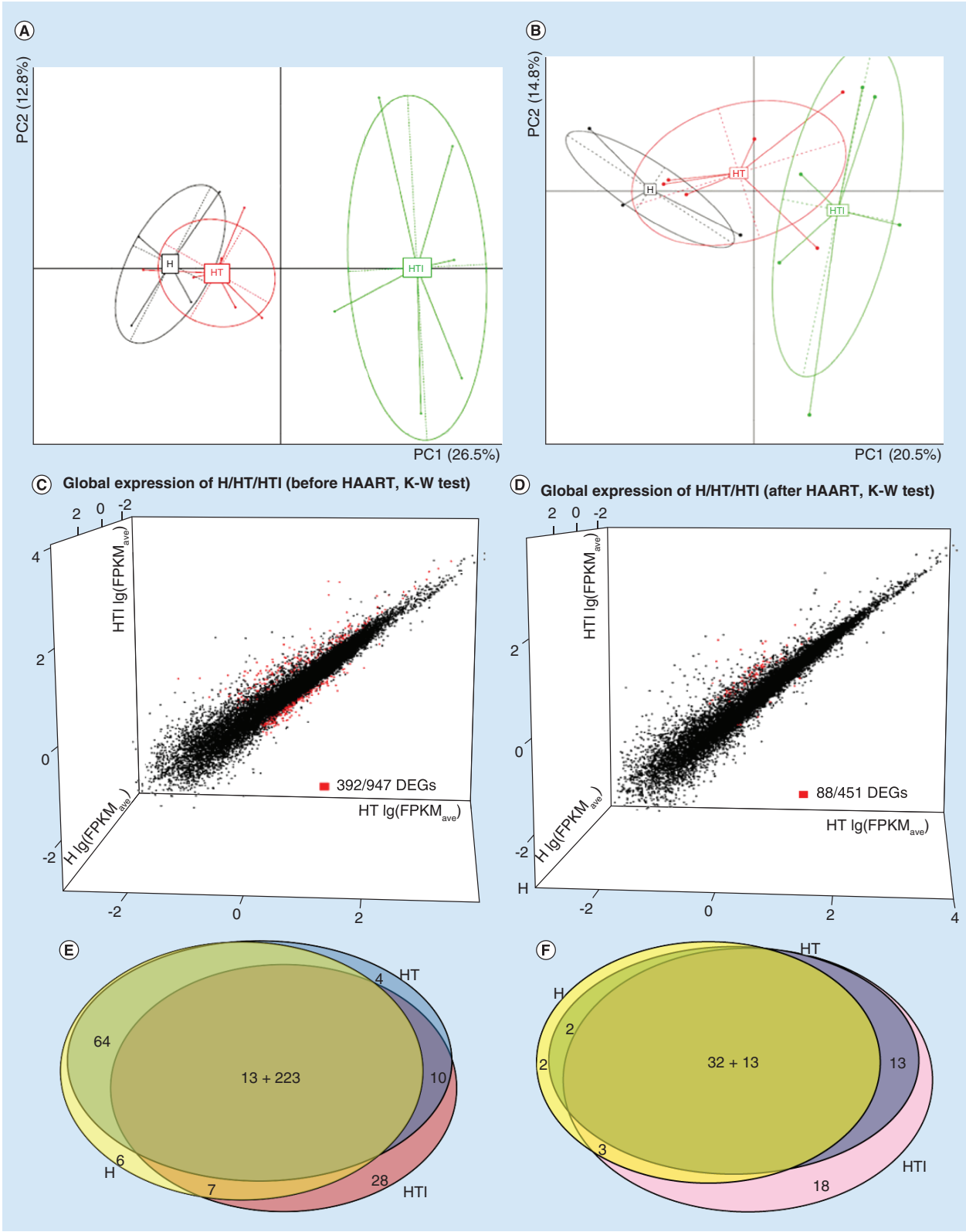

Figure 1. Global gene expression features among different groups.

Principal component analysis based on FPKM values of each samples for each sample before **(A)** and after **(B)** HAART. Red: HT group; black: H group and green: HTI group. RNA-seq global expression level of genes by Cuffdiff before **(C)** and after **(D)** HAART for all three groups. Genes marked in red represent significant DEGs (between HT and HTI group) whose expression level of genes passed the K–W significance test with the H group added in. Point coordinates were determined by log (average FPKM) in each group, respectively. The overlap of red represented significant DEGs (presence in at least 70% of samples) between different groups were layout as Venn diagram before **(E)** and after **(F)** HAART.

DEG: Differentially expressed gene; FPKM: Fragments per kilobase million; H: HIV$^+$; HAART: Highly active antiretroviral therapy; HT: HIV-TB$^+$; HTI: HIV-TB$^+$ with IRIS; IRIS: Immune reconstitution inflammatory syndrome; K–W: Kruskal–Wallis.

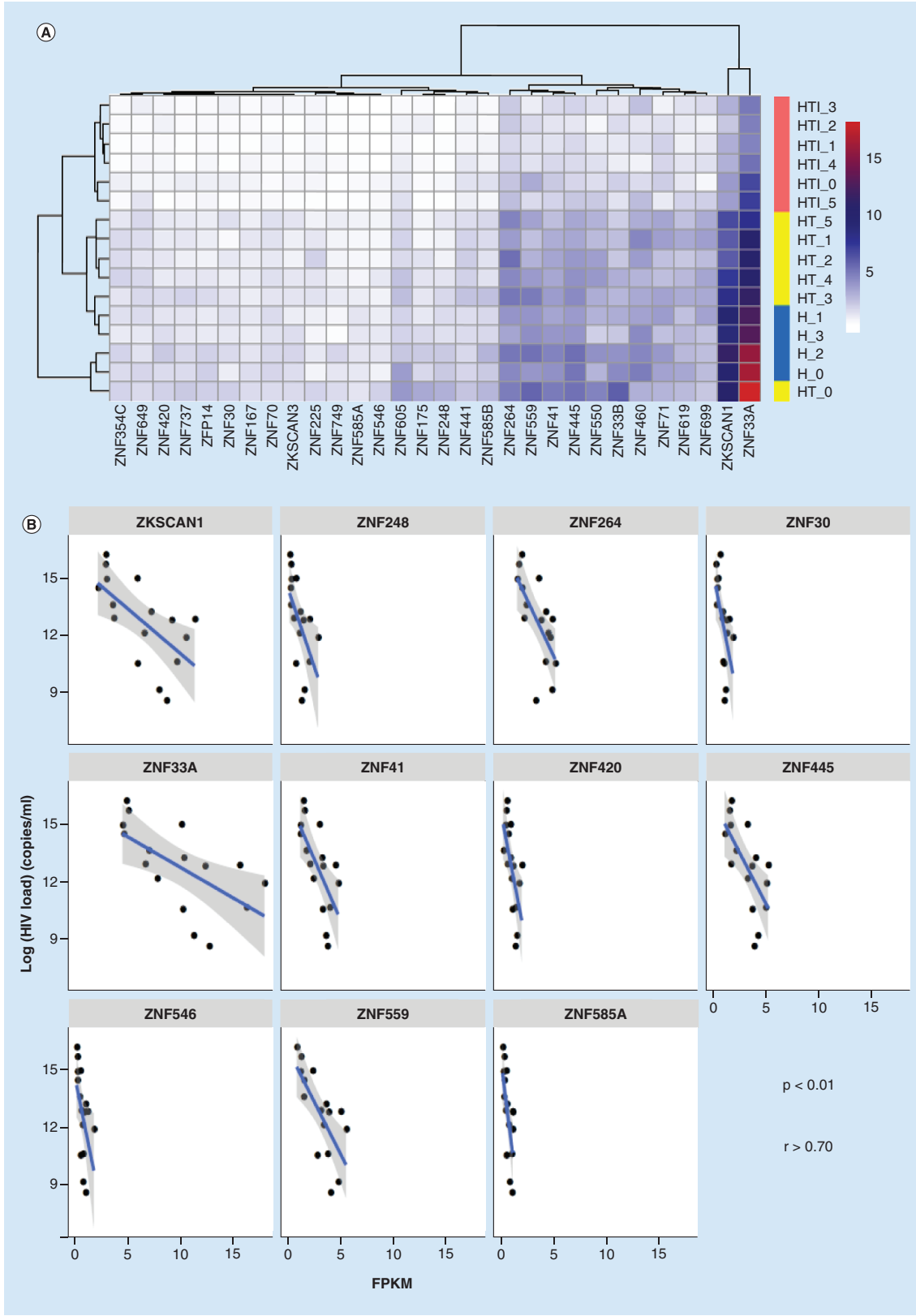

Figure 2. Expression levels of *ZNF* genes expression and its correlation with HIV-RNA load.
(A) Heatmap of 30 ZNF genes expression of Generic Transcription Pathway. High expression (red) gene and low expression (white) gene determined by their FPKM values. **(B)** The Spearman correlation (r) of ZNF expression and log (HIV-RNA load). **(C)** Expression level of several ZNF genes. The red and blue boxes separately represent the FPKM value before and after HAART. All are differentially expressed among three groups before HAART (K–W test: $p < 0.01$; FDR < 0.05).
FDR: False discovery rate; FPKM: Fragments per kilobase million; HAART: Highly active antiretroviral therapy; K–W: Kruskal–Wallis.

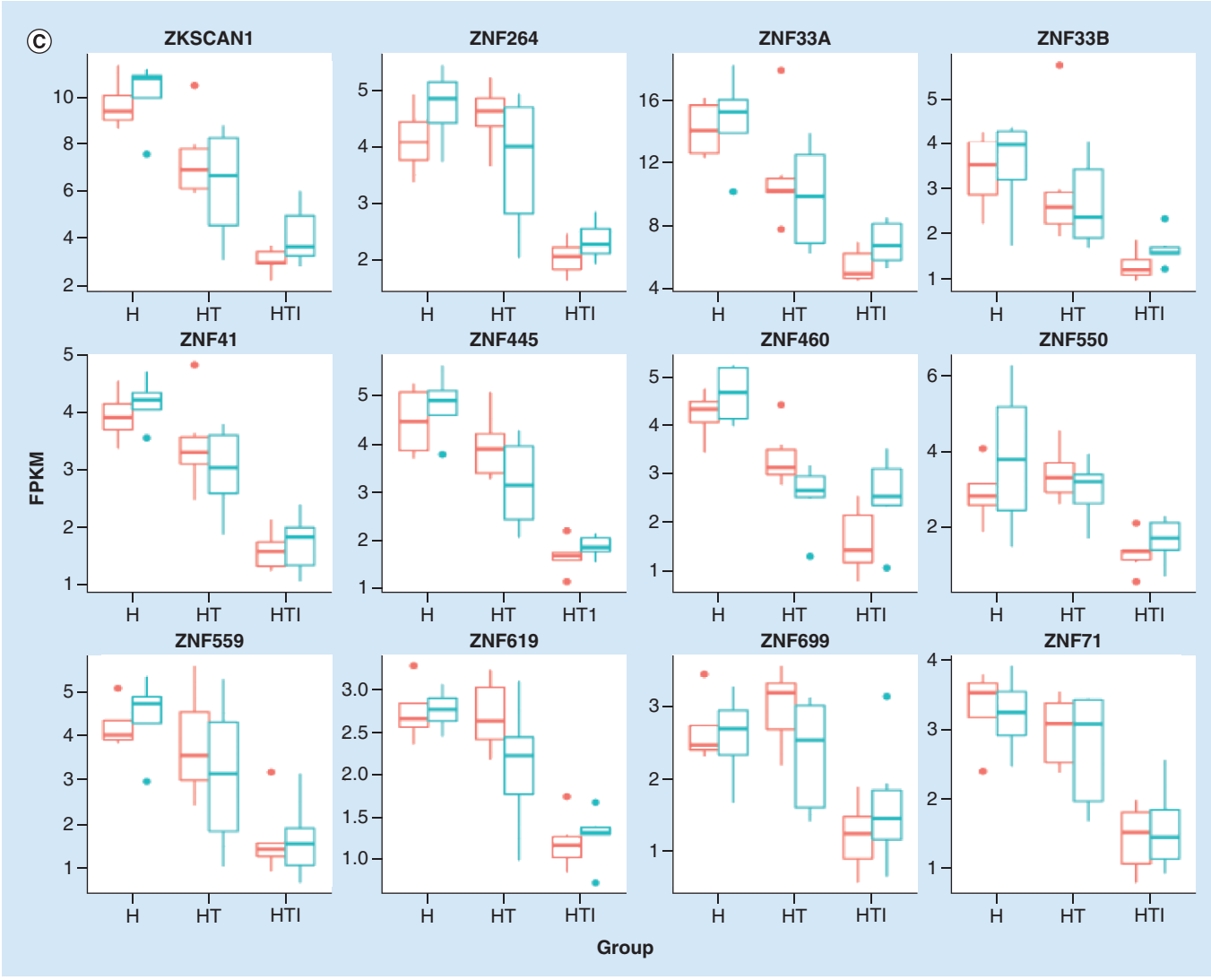

Figure 2. Expression levels of *ZNF* genes expression and its correlation with HIV-RNA load (cont.).
(A) Heatmap of 30 ZNF genes expression of Generic Transcription Pathway. High expression (red) gene and low expression (white) gene determined by their FPKM values. **(B)** The Spearman correlation (r) of ZNF expression and log (HIV-RNA load). **(C)** Expression level of several ZNF genes. The red and blue boxes separately represent the FPKM value before and after HAART. All are differentially expressed among three groups before HAART (K–W test: $p < 0.01$; FDR < 0.05).
FDR: False discovery rate; FPKM: Fragments per kilobase million; HAART: Highly active antiretroviral therapy; K–W: Kruskal–Wallis.

groups (Figure 2C & Supplementary Figure 3). Only ZNF225 in HT group and ZNF749 in HTI group showed a significant difference before and after HAART (Rank test, $p < 0.05$), most of these *ZNF* genes were stable before and after HAART (Supplementary Figures 2 & 3).

Functional domain analysis was conducted to see whether the extra unidentified ZNF proteins could share a common domain and probably have the same function. The results showed that among 30 ZNF genes enriched in Generic Transcription Pathway, 27 of them (except ZNF619, ZNF70 and ZNF71) belonged to Cys2His2 type zinc finger protein with a Krueppel-associated box (KRAB) domain (Table 4). The C_2H_2-like fold group is by far the best-characterized class of zinc fingers and is extremely common in mammalian transcription factors. The number of zinc fingers in each ZNF protein varied from five to 19. Previous studies have pointed out that *ZNF* genes with a KRAB domain can inhibit HIV proliferation; this matched the results of minus correlation coefficient between HIV RNA load and FPKM of *ZNF* genes (before HAART). In this study, we have shown that the maximal correlation coefficient was nearly up to -0.78 (ZNF559), and 19 of 26 *ZNF* genes were up to about -0.6, which

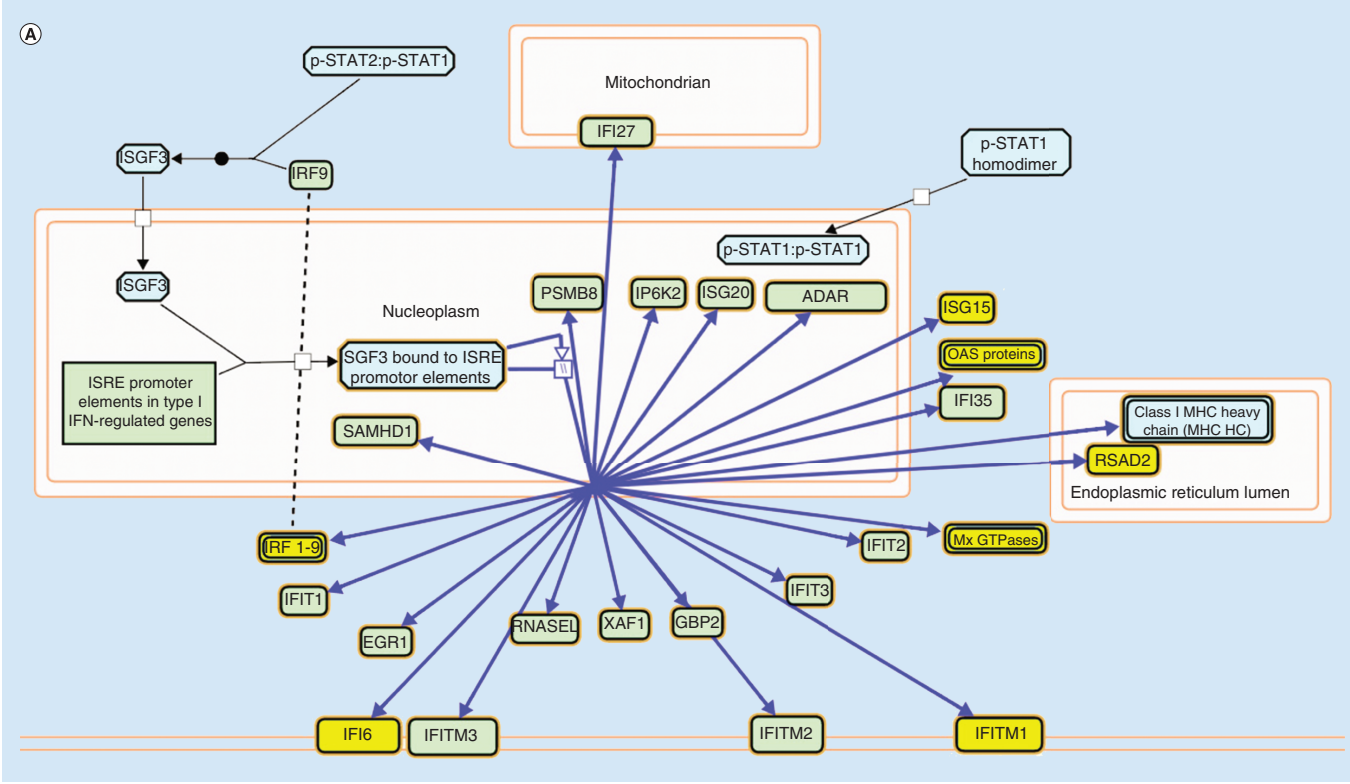

Figure 3. I nterferon-stimulated genes pathway and genes expression level.
(A) Expression of IFN-induced genes in IFN-α/β-signaling pathway (from Reactome). Yellow boxes represent DEGs, which were found in our data. **(B)** FPKM values of six genes enriched in the α/β-signaling pathway. The red and blue boxes separately represent the FPKM values before and after HAART (K–W test in three groups, *p < 0.05, **p < 0.01; Wilcoxon Rank Sum Test in before/after,*p < 0.05, **p < 0.01).
DEG: Differentially expressed gene; FPKM: Fragments per kilobase million; HAART: Highly active antiretroviral therapy; IFN: Interferon; K–W: Kruskal–Wallis.

indicates the potentially negative correlation between *ZNF* genes expression level and HIV RNA load (Figure 2B & Supplementary Table 5). Although three *ZNF* genes (ZNF70, ZNF619, ZNF71) with no KRAB domain also showed little correlation with HIV load, the p-value was high (Supplementary Table 5). This further suggests that the *ZNF* genes identified in our study may inhibit the proliferation of HIV to some extent, but functional studies on how HIV is able to overcome this antiviral modality alone or in combination with mycobacteria with the deteriorating immune system are sorely needed to cement this observation.

Interferon-stimulated genes like *ISG15* were significantly expressed before HAART in the HTI group

For the comparison between before and after time points in the HT group, 36 DEGs were identified (28 up-regulated, eight down-regulated), whereas for the comparison of HTI group (before and after HAART), 74 DEGs were identified (50 up-regulated, 24 down-regulated). As we questioned why in some HIV patients IRIS occurs after HAART, our subsequent analysis was focused on the comparison between before and after treatment time points mainly in the HTI group. The DE genes before and after in the HT and the HTI groups were identified, however, the number of overlapping genes between the two groups was only three (IFI44L, RSAD2, USP18) and the expression pattern was greatly different in two groups (Figure 3B). For example, in the HT group, the gene *RSAD2* and *USP18* were identified to be differentially expressed by Cuffdiff before and after HAART, while the Wilcoxon Rank Sum Test result did not show significant difference. In contrast, both methods showed a significant difference for the three genes before and after HAART for the HTI group. Furthermore, the fold-change of these genes suggested that the downregulation before and after HAART was higher in the HTI group, as opposed to both H and HT groups (Figure 3B).

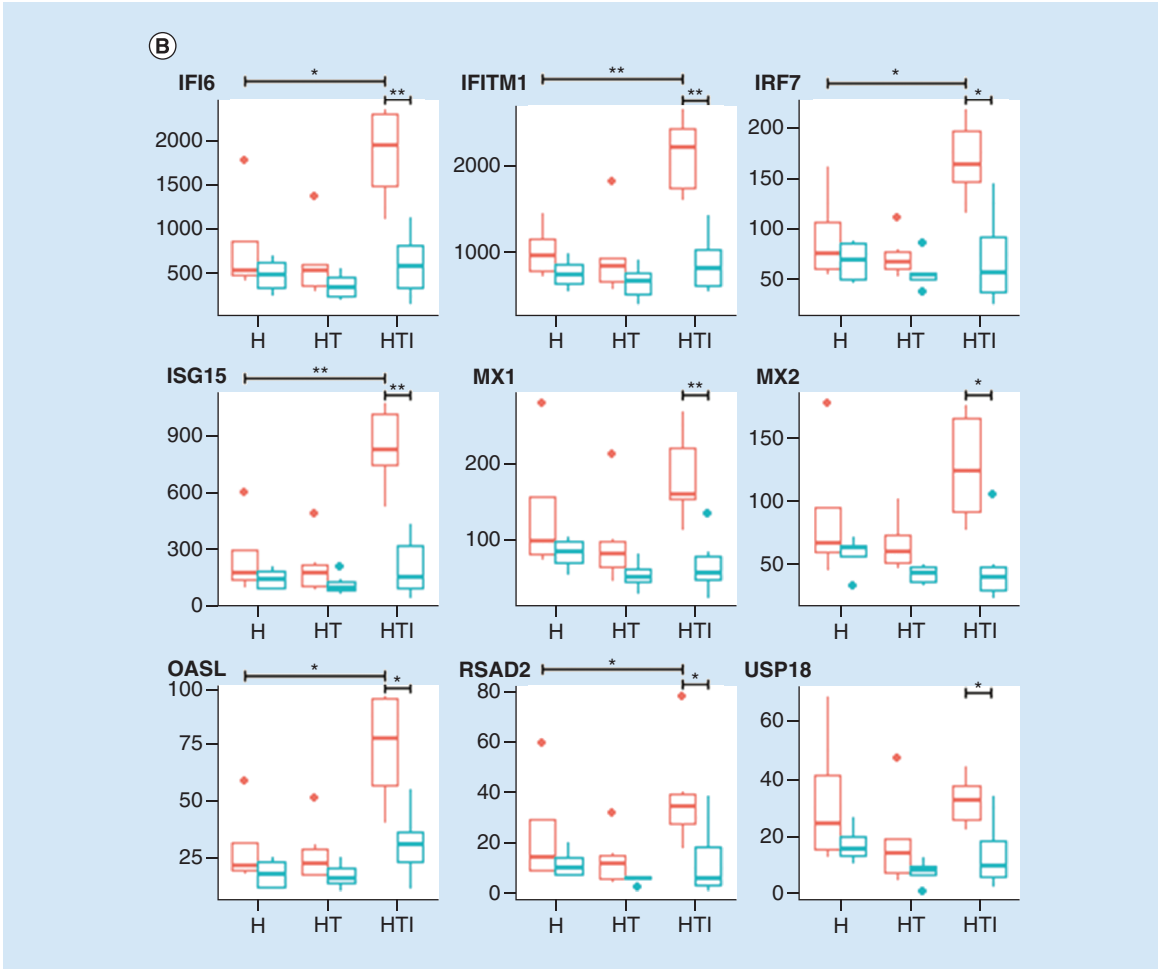

Figure 3. I (cont.). nterferon-stimulated genes pathway and genes expression level.
(A) Expression of IFN-induced genes in IFN-α/β-signaling pathway (from Reactome). Yellow boxes represent DEGs, which were found in our data. **(B)** FPKM values of six genes enriched in the α/β-signaling pathway. The red and blue boxes separately represent the FPKM values before and after HAART (K–W test in three groups, *$p < 0.05$, **$p < 0.01$; Wilcoxon Rank Sum Test in before/after,*$p < 0.05$, **$p < 0.01$).
DEG: Differentially expressed gene; FPKM: Fragments per kilobase million; HAART: Highly active antiretroviral therapy; IFN: Interferon; K–W: Kruskal–Wallis.

Finally, all these 72 DEGs derived from the HTI group were retained for pathway analysis using TargetMine. In pathway analysis, nine of 72 DEGs (two genes were undefined, Supplementary Tables 6 & 7) from the HTI group were significantly enriched in the IFN-α/β-signaling pathway (Figure 3A, p-value = 1.35×10^{-7}, Holm-Bonferroni [H-B] correction). Enriched genes were *IFI6, IFITM1, IRF7, ISG15, MX1, MX2, OASL, RSAD2* and *USP18*, respectively. Before HAART, FPKM values of several interferon-stimulated genes (ISGs; ISG15, IRF7 and MX2) were substantially higher in the HTI group than in the H and HT groups (Figure 3B, K–W test). We also observed that after the initiation of HAART treatment, the FPKM values of *IFI6, IFITM1, IRF7, ISG15, MX1, OASL* decreased sharply [32] (Figure 3B, p-value < 0.05, Wilcoxon Rank Sum test).

Other pathways that were significantly enriched by TargetMine were in the cytokine-related pathways (Supplementary Table 8), such as cytokine signaling in immune system (p-value = 1.1×10^{-3}, H-B correction) and cytokine–cytokine receptor interaction (p-value = 1.9×10^{-2}, H-B correction). After the initiation of HAART, the expression level of genes enriched in these pathways was relatively higher than in the before therapy group, which was consistent with the previous microarray-based study [18,33].

The GSEA [30] for the H, HT and HTI groups showed that 29 (nine up-regulated), 26 (15 up-regulated) and nine (eight up-regulated) DEG sets changed in all three groups following HAART (Supplementary Table 9), and

in the groups H and HT, a higher overlap was observed for both up- and down-regulated gene sets (nine up and nine down), a reflection of which could be seen in the PCA (Figure 1B). Among the down-regulated gene sets, all three groups shared the IFN-α/β-signaling gene sets with a different Normalized Enrichment Score (HTI = -2.5, HT = -1.97, H = -2.16), which showed significant decrease particularly in the HTI group and concurred with the results of pathway analysis (Figure 3A & B). Among the nine down-regulated overlapping gene sets in the H and HT groups, we found some gene sets related to cell cycle and mitosis, such as G2/M checkpoints and cell cycle mitotic activity. Previous studies have shown that HIV-type 1 vpr gene could arrest infected T cells in the G2/M phase of the cell cycle [34]. HIV LTR has high activity in the G2 phase of the cell cycle for its own benefit. After the initiation of HAART, these gene sets related to cell cycle were significantly down-regulated, which revealed a positive effect of HAART in both H and HT groups. Besides, we also observed that gene sets related to protein synthesis were up-regulated to varying degrees, such as 3-UTR-mediated translational regulation and peptide chain elongation in the H and HT groups, whereas transport to the Golgi and subsequent modification and transport of mature mRNA derived from an intron less transcript in the HTI group. Although the gene sets did not overlap between H/HT and HTI groups, they indirectly showed enhancement in the protein synthesis activity following the initiation of HAART suggesting reconstitution of the immune system.

We also found 451 genes were differentially expressed after HAART between HT and HTI groups (Supplementary Figure 1C). With FPKM value of H group added in, K–W one-way significance test was performed to select out the final 88 significant DEGs (seven down-regulated, 81 up-regulated in the HTI group, Figure 1D, Supplementary Table 10). Pathway analysis-enriched genes in cell cycle, mitosis and cell cycle checkpoint-related pathways, and all these genes were down-regulated in the HT group when compared against the HTI group (Supplementary Table 11), which was consistent with the GSEA results.

The potential difference in the TB content between HTI & HT groups

Using the 392 DEGs identified in the pathway analysis for GO (gene ontology) enrichment in biological process by TargetMine ($p < 0.05$, H-B correction), the most significant GO was rooted in the defense response to bacterium (Figure 4A). Sixteen genes enriched in this pathway segregated the HTI, HT and H groups based on expression profiles. We observed that except for the *TLR9* gene in the HTI group, the expression levels of other genes were significantly higher than the other two groups ($p < 0.01$, K–W test). Among these genes, the *S100A8/S100A9* genes, also called *MRP8/14* (Figure 4B), coding for calprotectin (a heterodimer of two calcium-binding proteins present in the cytoplasm of neutrophils and expressed on the membrane of monocytes [35]) were observed. Other relatively significant GO terms were also related to RNA synthesis and transcription, similar to the results of Pathway Enrichment mentioned above, which occurred at the initiation of HAART suggesting some genomic difference at the transcriptional level between HT and HTI groups.

Marais *et al.* have shown that 2 weeks after the initiation of ART, compared with MTB non-IRIS patients, S100A8/S100A9 was significantly increased in TBM (tuberculous meningitis)-IRIS patients [15]. Together with our findings on the expression level of S100A8/S100A9, the expression of these two genes was also higher in the HTI group, and it also increased following HAART.

Discussion

This study shows a systematic deep-sequencing transcriptomic analysis, using RNA-seq technology, of the TB-IRIS patients and shows the possible genomic basis of it. We found that ZNFs and ISGs were intrinsically involved in TB-IRIS. To explain the intrinsic association between ISGs and ZNF genes, it is worthy of mentioning that the ISGs demonstrated a synergistic antiviral activity with zinc-finger antiviral protein (ZAP), and multiple ISGs synergize with the ZAP to mediate anti-alphavirus activity [36]. We believe this could be one explanation for our observations, as both ISGs and zinc-finger gene enrichment was seen in our data, yet it is difficult to determine how each of the ISGs and ZNF genes synergize and recover following HAART to maintain intrinsic association between them in countering HIV and Mycobacterial infection in the face of deteriorating immune system. Many ISGs play function more antiviral effectively in the presence of zinc finger that suggests in addition to possible direct interactions with the individual ISGs, ZNF genes function by altering the intracellular milieu in a manner. But whether the seamless communication between ISGs and ZNF remains intact upon the development of IRIS is reflected in the unique genes in cellular processes guiding the cellular integrity that we observed in the HTI group.

In respect to ZNF genes, it is noteworthy that previous studies have revealed that some ZNF proteins (i.e., ZNF10, ZNF175 [37,38]) could effectively inhibit the proliferation of HIV through the interaction with NF-κB and Sp1-

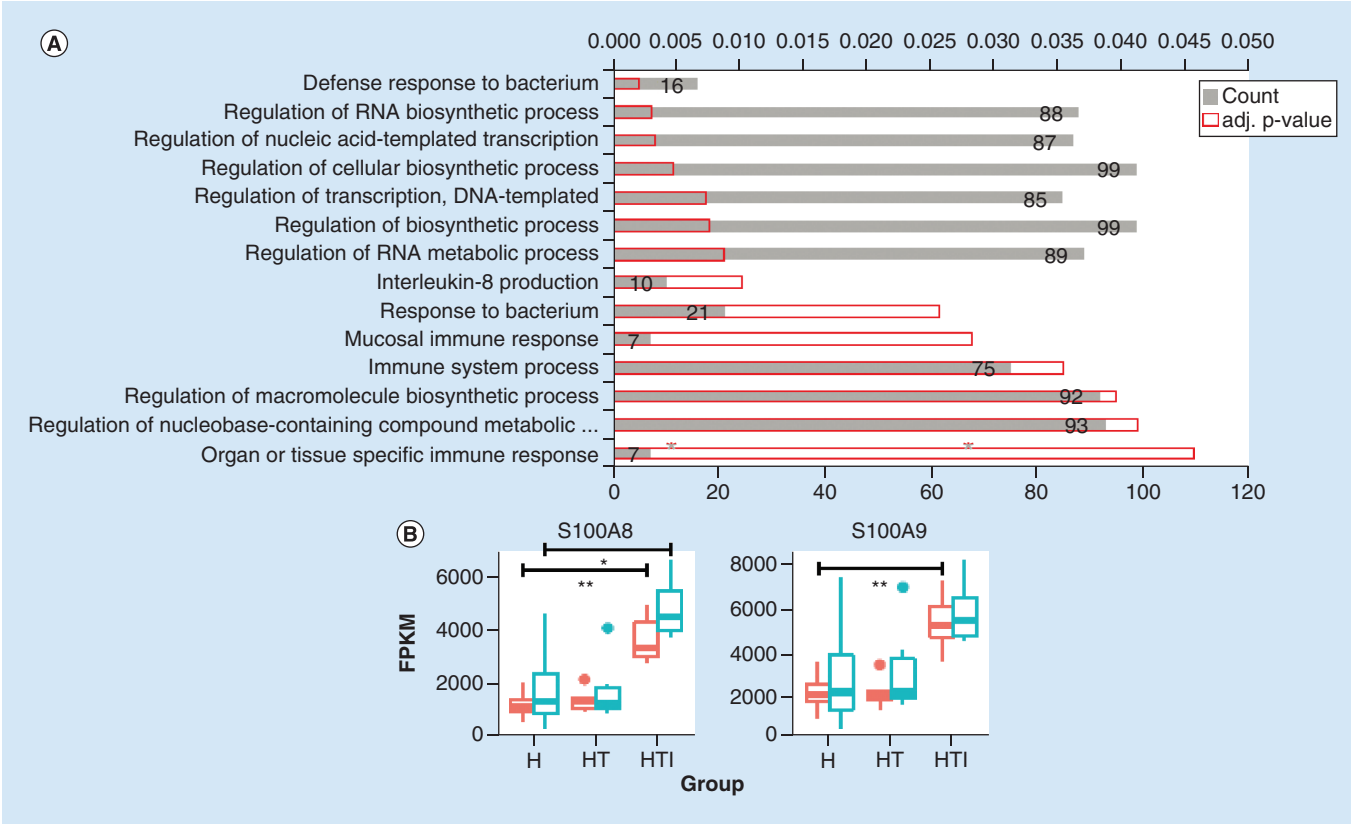

Figure 4. GO enrichment and S100A8/S100A9 calprotectin genes.
(A) GO enrichment of DEGs in biological process. The number bar of genes in GO were list below and the enrichment p-value bar were list above. **(B)** FPKM values of S100A8/S100A9 before (red) and after (blue) HAART (*p < 0.05, **p < 0.01, K–W test). Significant difference could be noticed among groups, but the effect of HAART was not obvious.
DEG: Differentially expressed gene; FPKM: Fragments per kilobase million; GO: Gene ontology; HAART: Highly active antiretroviral therapy; K–W: Kruskal–Wallis.

binding motifs [39], and the ZAP could inhibit HIV-1 by recruiting both the 5′- and 3′-mRNA degradation machinery to specifically degrade multiply spliced HIV-1 mRNAs [40]. Yet other studies have shown that ZNF proteins (hZNF 134) could, on the contrary, promote HIV replication [41]. In our analysis of the *ZNF* genes identified, the motif of ZNF175 (or OTK18) overlapped with this study that showed the motif functionally to inhibit HIV replication. Although the expression of ZNF genes is strongly functionally correlated, the function of other ZNF genes identified in our study remains to be elucidated [42]. Supporting this argument, recently the hZNF134 has been shown to promote viral replication during coinfection with HIV and Mycobacteria [22]. Although hZNF134 was not observed in our study, it does suggest a similar modality taking place during the infection process with other *ZNF* genes we have found enriched, and whose roles remain unclear.

Furthermore, to put this in the context of ZNF synergy with the ISGs, we found significant correlation between before and after HAART functional expression levels of ISGs in the HIV-TB-IRIS group, which decreased sharply in contrast to the H and HT groups, where the expression levels were maintained at lower levels. Supporting this, there was concomitant decline in the gene expression of ZNFs in the HTI group, which also showed considerable variability pre- and post-HAART. Thus, despite the enrichment of ISGs and ZNFs, this lack of synergy could be a consequence of their declining expression in the HTI group coupled with the immunological imbalance between them, in which HAART fails to restore in the face of crumbling immune system. Alternatively, it is likely that ISGs go up and ZNFs decline means that ZNFs no longer leave the cells permissible to ISG function. In the light of these observations, the involvement of Mycobacterium infection, accompanied by considerable deterioration of the immune system and factors that govern cellular integrity, which is reflected in imperfect recovery in patients' $CD4^+$ T-cell counts and plasma viremia following HAART. Thus, the imbalance and diminishing trends of both ZNFs and ISGs after HAART could act as vital factors in determining the effectiveness of the seamless synergy

ZNF and ISGs maintain in a healthy immune system. To reinforce this idea, previous studies have pointed out that *ISG15* gene could inhibit the release of HIV from cells [43] and *IFITM1* [44] gene inhibits viral replication and proliferation [45] and also affects the expression levels of IRF7, MX2, OAS1, which are associated with $CD4^+$ T-cell count and plasma HIV viral load [46]. These were among the nine significant ISGs identified in our study, cementing their functional significance.

Thus, looking into the nature of genes that makes the HTI group unique, we found that this was guided by the genes that govern cellular integrity related to DNA, chromosome, microtubule, leukocyte migration, actin, cell adhesion and proliferation, and so forth. In light of these observations, we hypothesize that the integrity of cellular processes may be impaired in the HTI group, and may possibly associate with IRIS, along with the loss of synergy between ISGs and ZNFs.

Based on the commonly accepted notion that there are no 'signature genes' in the $CD4^+$ cells [47], in our data also, there was no significant correlation between $CD4^+$ T-cell number and most (38/38 in H group, 37/38 in HT group, 34/38 in HTI group) ZNF DEGs (38 ZNF DEGs that enriched in Generic Transcription Pathway, Supplementary Table 4). Up- or downregulations of these ZNF genes mentioned above did not follow the increase of $CD4^+$ T-cell numbers in different patients, suggesting that the Generic Transcription Pathway was truly the difference.

Another feature of our study was the high expression of S100A8/S100A9 genes in the HTI group before HAART. Both pro- and anti-inflammatory properties reported for these proteins are involved in activating TLR4 responses. It functions by binding the receptors (RAGE, TLR4) in the membrane, activating and mediating the inflammatory signaling pathway and biological process. S100A8 and S100A9 can function separately, likely through distinct receptors but a systematic comparison of their effects *in vivo* is limited. Previous studies have shown that the S100A8 protein has a regulatory effect in inflammatory signal transduction. *In vitro* proinflammatory factors, such as LPS, TNF and IL-1 could induce S100A8 expression in macrophages and endothelial cells [48–50]. S100A8 could stimulate inflammatory cells to release factors, directly get involved in the inflammatory process [51]. Other studies have also revealed that S100A8 protein can help treat traumatic inflammation [52]. *In vitro* S100A8/S100A9 could nonspecifically bind cytokines like IL-1β, IL-6 and TNF-α. Moreover, it can also inhibit expression of some inflammatory cytokines at the gene level [53]. In our data, after HAART, no significant upregulation of S100A8/S100A9 gene was noticed, but an upregulation of an anti-inflammatory cytokine (IL-10) and a series of receptors (IL7R, CCR4, Supplementary Table 8) after HAART was observed, which possibly resulted in immunological imbalance, and may be one of the reasons for the development of TB-IRIS. It is to be noted that S100A8 induction is IL-10 dependent [54], regulated in a manner similar to the *IL-10* gene, but S100A9 has no effect on this, suggesting that these genes also work separately in governing the pro- and anti-inflammatory cytokine expression.

Furthermore, it is important to iterate that previous studies have shown that patients with active TB had significantly increased plasma levels of calprotectin compared with pulmonary sarcoidosis and healthy controls [35]. Supporting this, it has also been shown that it augments *MTB* growth in a dose- and time-dependent manner [55]. Schwartz *et al.* have shown that in HIV disease, dysregulated neutrophil responses to endotoxins stimulation and S100A8/A9 inhibition may contribute to a higher risk for oxidative stress-associated ailments [56]. Then, elevated serum levels of S100A8, S100A9 and their heterocomplex calprotectin have been reported in association with HIV infection, especially during disease exacerbation [57].

Based on our observations, higher expression levels of *S100A8/S100A9* in the IRIS (HTI group) tend to favor TB infection and replication, suggesting that after anti-TB therapy, an inconspicuous state of a more severe infection of TB exists in the HTI group that TB-IRIS arises from a combination of a high MTB antigen load at ART initiation [3] and differential antigen recognition and immune signaling by innate immune receptors after ART initiation in TB-IRIS patients, which in turn contributes to hypercytokinemia and inflammation. We believe this could be a hidden factor for the breakaway of IRIS after HAART. Whether increased S100A8/A9 levels in association with inflammation or infection, contribute to enhanced immune response as suggested by some [58] or instead, represent a native anti-inflammatory process as suggested by others [59] remain to be fully elucidated.

In light of these observations, we hypothesize one of possible mechanistic models for the occurrence of IRIS (Figure 5). Before HAART, among the HIV-TB-coinfected patients, low expression levels of ZNF genes were observed. It is notable that some ZNF-encoded proteins show the ability to inhibit HIV proliferation. But due to some self- and cellular integrity defects coupled with weaker synergy between ISGs and zinc finger genes in mounting antiviral effect may impair this inhibitory activity, causing higher HIV RNA load in the blood and

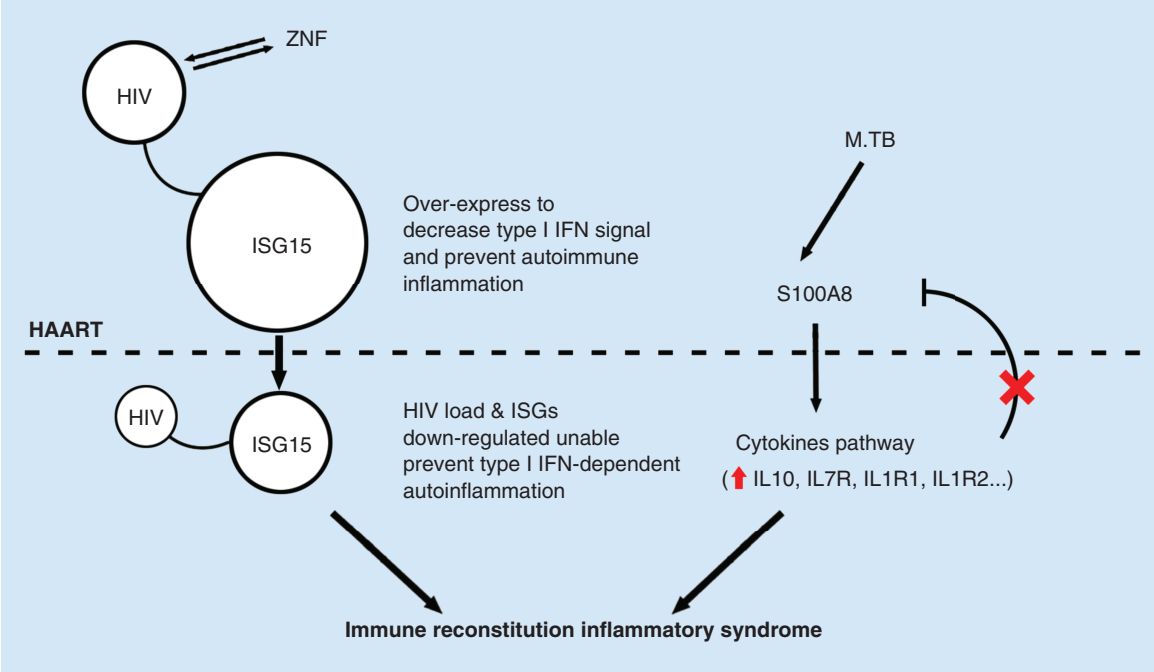

Figure 5. Proposed model for the underlying pathogenetic mechanism for the development of immune reconstitution inflammatory syndrome.

poor sequestration of immune cells and imperfect control of viremia. Thus, for these patients, their relatively low immunity with less $CD4^+$ T-cell could not effectively attack the *Mycobacterium* existing in their bodies due to excessive HIV load possibly stimulating expression of ISGs (i.e., ISG15) [46,60], causing them to overexpress in order to compensate for the low expression of ZNF genes.

After the initiation of HAART, the HIV RNA load decreased and the expression of *ISG15* gene also declined, which is consistent with a recent study of time points before and after HAART in HIV patients [61]. Researches have pointed out that *ISG15* gene had the anti-inflammatory effect, and low expression of *ISG15* gene could cause low-level USP18, triggering the generation of type I IFN and increase of the signal function and prompt the occurrence of autoinflammation [62]. A recent study of cytokine in the HTI patient group showed that following the initiation of HAART, cytokines and proinflammatory factors were up-regulated, which could promote autoinflammation [33]. The excessive immune response together with the inflammation further exacerbated the reaction of IRIS. Moreover, the inflammation that affects the regulative ability and the expression of S100A8/S100A9 may act as a contributory factor for the development of IRIS in HIV/TB patients.

Marais *et al.* have shown that 2 weeks after the initiation of ART, a high baseline MTB antigen load drives an inflammatory response that manifests clinically as TBM-IRIS in most, but not all, patients with TBM. Neutrophils and their mediators, especially S100A8/A9, are closely associated with the central nervous system inflammation that characterizes TBM-IRIS [15]. Thus, together with our findings on the expression level of S100A8/S100A9, we believe that for the HIV/TB coinfection patients, higher expression level of S100A8/S100A9 appears to favor TB infection, replication and occurrence of TB-IRIS.

Conclusion

Our result is showing the possible genomic basis of TB-IRIS, which revealed that genes of ZNF and interferon-stimulating families were important in the inhibition of HIV replication. Through their expression in the three groups, we were able to visualize functional synergies that evolve differently as the immune system deteriorates. These findings have laid a foundation for the gene expression levels to be used as a classifier for predisposition to TB-IRIS, but more data are needed on larger number of patients. While the expression of ZNF genes may be an important factor for AIDS patients for defining the initiation time of HAART, their synergy with the ISGs is of paramount importance in mounting an antiviral effect and maintenance of the immune system during HAART, as

its antiviral activity heavily relies on the health of the immune system. These data propose a possible pathogenetic mechanism and show the first snapshot of the genomic basis of TB-IRIS, which may lay a strong foundation for the development of new generation of genomic biomarkers leading to better treatment strategies for HIV-TB-IRIS.

Summary points

- There is possible genomic basis of TB-immune reconstitution inflammatory syndrome (IRIS) which revealed that genes of ZNF and interferon-stimulating families were important in the inhibition of HIV replication.
- Significant differential lower expression of ZNF genes in TB-IRIS groups regardless of before or after highly active antiretroviral therapy (HAART) although it changed little after HAART.
- There is negative relationship between ZNF genes' expression and HIV virus load before HAART in all groups before HAART.
- The differentially expressed ZNF genes which with a Krueppel-associated box domain enriched in Generic Transcription Pathway.
- Interferon-stimulated genes like *ISG15* were significantly higher expressed before HAART in the HIV-TB^{+} with IRIS group but dropped quickly after HAART.
- For the differentially expressed genes between IRIS and non-IRIS groups, the most significant GO enrichment was rooted in the defense response to bacterium.
- The TB-associated gene *S100A8*/*S100A9* is expressed higher in TB-IRIS group before HAART, which leads the potential IRIS development.
- There is a possible pathogenetic mechanism and shows the first snapshot of the genomic basis of TB-IRIS, which may lay a strong foundation for the development of new generation of genomic biomarkers leading to better treatment strategies for HIV-TB-IRIS.

Availability of data & material

Please contact author for data requests. It can be deposited in GenBank, if required.

Acknowledgements

The authors thank all the patients for consenting their blood samples for our research study, and clinicians for assisting with blood collection and clinical profiles.

Authors' contributions

K Kristiansen, H Wang and Y Liu designed the experiments. J Ma, W Su, Q Li and J Ji analyzed the sequenced data and wrote the manuscript. F Zhao and Y Deng collected all the samples and prepared them for sequencing. J Li, Y Deng and X Wang assisted in the data analysis. Y Zhou, X Wang, H Yang, N Saksena and K Kristiansen assisted in manuscript preparation.

Financial & competing interests disclosure

This study was supported by the Science and Technology Innovation Foundation of Shenzhen (grant no. JCYJ20150402111430645) and Shenzhen Municipal Government of China (no. JCYJ20160427151920801). The authors have no other relevant affiliations or financial involvement with any organization or entity with a financial interest in or financial conflict with the subject matter or materials discussed in the manuscript apart from those disclosed.

No writing assistance was utilized in the production of this manuscript.

Ethical conduct of research

The study protocol was approved by the Institutional Review Board of the Shenzhen Third People's Hospital. Written informed consent was obtained from all participants. All methods were performed in accordance with the relevant ethical guidelines and regulations.

Supplementary data

To view the supplementary data that accompany this paper please visit the journal website at: www.futuremedicine.com/doi/full/10.2217/pme-2017-0084

References

Papers of special note have been highlighted as: • of interest; •• of considerable interest

1 Sepkowitz KA. AIDS–the first 20 years. *N. Engl. J. Med.* 344(23), 1764–1772 (2001).

2 Ryndak MB, Singh KK, Peng Z *et al.* Transcriptional profiling of Mycobacterium tuberculosis replicating *ex vivo* in blood from HIV- and HIV+ subjects. *PLoS ONE* 9(4), e94939 (2014).

3 Lai RP, Meintjes G, Wilkinson RJ. HIV-1 tuberculosis-associated immune reconstitution inflammatory syndrome. *Semin. Immunopathol.* 38(2), 185–198 (2015)

4 French MA, Price P, Stone SF. Immune restoration disease after antiretroviral therapy. *AIDS* 18(12), 1615–1627 (2004).

5 WHO. Global tuberculosis report 2017. (2017). www.who.int/tb/publications/global_report/en/

• **Authoritative report about tuberculosis infection around the world with comprehensive and regular updates**

6 Gibson P, Abramson M. *Evidence-Based Respiratory Medicine.* BMJ Books/Blackwell Pub., Malden, Mass, USA (2005).

7 Palella Jr FJ, Delaney KM, Moorman AC *et al.* Declining morbidity and mortality among patients with advanced human immunodeficiency virus infection. *N. Engl. J. Med.* 338(13), 853–860 (1998).

8 Zheng Y, Zhou H, He Y, Chen Z, He B, He M. The immune pathogenesis of immune reconstitution inflammatory syndrome associated with highly active antiretroviral therapy in AIDS. *AIDS Res. Hum. Retroviruses* 30(12), 1197–1202 (2014).

9 French MA, Mallal SA, Dawkins RL. Zidovudine-induced restoration of cell-mediated immunity to mycobacteria in immunodeficient HIV-infected patients. *AIDS* 6(11), 1293–1298 (1992).

• **First report of the TB-HIV-immune reconstitution inflammatory syndrome (IRIS), which caused people to give more attention to highly active antiretroviral therapy.**

10 Bourgarit A, Carcelain G, Martinez V *et al.* Explosion of tuberculin-specific Th1-responses induces immune restoration syndrome in tuberculosis and HIV co-infected patients. *AIDS* 20(2), F1–F7 (2006).

11 Meintjes G, Wilkinson KA, Rangaka MX *et al.* Type 1 helper T cells and FoxP3-positive T cells in HIV–tuberculosis-associated immune reconstitution inflammatory syndrome. *Am. J. Respir. Crit. Care Med.* 178(10), 1083–1089 (2008).

12 Bourgarit A, Carcelain G, Samri A *et al.* Tuberculosis-associated immune restoration syndrome in HIV-1-infected patients involves tuberculin-specific CD4 Th1 cells and KIR-negative γδ T cells. *J. Immunol.* 183(6), 3915–3923 (2009).

13 Conradie F, Foulkes AS, Ive P *et al.* Natural killer cell activation distinguishes Mycobacterium tuberculosis-mediated immune reconstitution syndrome from chronic HIV and HIV/MTB coinfection. *J. Acquir. Immune Defic. Syndr.* 58(3), 309–318 (2011).

14 Pean P, Nerrienet E, Madec Y *et al.* Natural killer cell degranulation capacity predicts early onset of the immune reconstitution inflammatory syndrome (IRIS) in HIV-infected patients with tuberculosis. *Blood* 119(14), 3315–3320 (2012).

15 Marais S, Wilkinson KA, Lesosky M *et al.* Neutrophil-associated central nervous system inflammation in tuberculous meningitis immune reconstitution inflammatory syndrome. *Clin. Infect. Dis.* 59(11), 1638–1647 (2014).

16 Andrade BB, Singh A, Narendran G *et al.* Mycobacterial antigen driven activation of CD14++CD16- monocytes is a predictor of tuberculosis-associated immune reconstitution inflammatory syndrome. *PLoS Pathog.* 10(10), e1004433 (2014).

17 Haddow LJ, Dibben O, Moosa MY, Borrow P, Easterbrook PJ. Circulating inflammatory biomarkers can predict and characterize tuberculosis-associated immune reconstitution inflammatory syndrome. *AIDS* 25(9), 1163–1174 (2011).

18 Tran HT, Van Den Bergh R, Loembe MM *et al.* Modulation of the complement system in monocytes contributes to tuberculosis-associated immune reconstitution inflammatory syndrome. *AIDS* 27(11), 1725–1734 (2013).

19 Maddocks S, Scandurra GM, Nourse C *et al.* Gene expression in HIV-1/Mycobacterium tuberculosis co-infected macrophages is dominated by M. tuberculosis. *Tuberculosis* 89(4), 285–293 (2009).

• **New achievements on TB-HIV-IRIS to detect macrophages.**

20 Hurd PJ, Nelson CJ. Advantages of next-generation sequencing versus the microarray in epigenetic research. *Brief. Funct. Genomics Proteomics* 8(3), 174–183 (2009).

21 Trapnell C, Roberts A, Goff L *et al.* Differential gene and transcript expression analysis of RNA-seq experiments with TopHat and Cufflinks. *Nat. Protoc.* 7(3), 562–578 (2012).

22 Chaussabel D, Pascual V, Banchereau J. Assessing the human immune system through blood transcriptomics. *BMC Biol.* 8(1), 84 (2010).

23 WHO. Treatment of tuberculosis: guidelines for national programmes. http://whqlibdoc.who.int/publications/2010/9789241547833_eng.pdf?ua=1

24 Fujie Z. China Free Antiretroviral Therapy Manual. People's Medical Publishing House (2012).

25 Meintjes G, Lawn SD, Scano F *et al.* Tuberculosis-associated immune reconstitution inflammatory syndrome: case definitions for use in resource-limited settings. *Lancet Infect. Dis.* 8(8), 516–523 (2008).

26 Zhao Z, Xu J, Chen J *et al.* Transcriptome sequencing and genome-wide association analyses reveal lysosomal function and actin cytoskeleton remodeling in schizophrenia and bipolar disorder. *Mol. Psychiatry* 20(5), 563–572 (2014).

27 Chen Y-A, Tripathi LP, Mizuguchi K. TargetMine, an integrated data warehouse for candidate gene prioritisation and target discovery. *PLoS ONE* 6(3), e17844 (2011).

28 Schurch NJ, Schofield P, Gierliński M *et al.* How many biological replicates are needed in an RNA-seq experiment and which differential expression tool should you use? *RNA* 22(6), 839–851 (2016).

29 Kim D, Pertea G, Trapnell C, Pimentel H, Kelley R, Salzberg SL. TopHat2: accurate alignment of transcriptomes in the presence of insertions, deletions and gene fusions. *Genome Biol.* 14(4), R36 (2013).

30 Subramanian A, Tamayo P, Mootha VK *et al.* Gene set enrichment analysis: a knowledge-based approach for interpreting genome-wide expression profiles. *Proc. Natl Acad. Sci. USA* 102(43), 15545–15550 (2005).

31 Ye J, Coulouris G, Zaretskaya I, Cutcutache I, Rozen S, Madden TL. Primer-BLAST: a tool to design target-specific primers for polymerase chain reaction. *BMC Bioinformatics* 13(1), 134 (2012).

32 Zahoor MA, Xue G, Sato H, Aida Y. Genome-wide transcriptional profiling reveals that HIV-1 Vpr differentially regulates interferon-stimulated genes in human monocyte-derived dendritic cells. *Virus Res.* 208, 156–163 (2015).

33 Lai RP, Meintjes G, Wilkinson KA *et al.* HIV-tuberculosis-associated immune reconstitution inflammatory syndrome is characterized by Toll-like receptor and inflammasome signalling. *Nat. Commun.* 6, 8451 (2015).

•• **New method of research on the TB-HIV-IRIS. This research finds some new achievements on diagnosis and prediction of the development of IRIS.**

34 Jowett JB, Planelles V, Poon B, Shah NP, Chen ML, Chen IS. The human immunodeficiency virus type 1 vpr gene arrests infected T cells in the G2 + M phase of the cell cycle. *J. Virol.* 69(10), 6304–6313 (1995).

35 Striz I, Trebichavsky I. Calprotectin - a pleiotropic molecule in acute and chronic inflammation. *Physiol. Res.* 53(3), 245–253 (2004).

36 Karki S, Li MM, Schoggins JW, Tian S, Rice CM, Macdonald MR. Multiple interferon stimulated genes synergize with the zinc finger antiviral protein to mediate anti-alphavirus activity. *PLoS ONE* 7(5), e37398 (2012).

37 Carlson KA, Leisman G, Limoges J *et al.* Molecular characterization of a putative antiretroviral transcriptional factor, OTK18. *J. Immunol.* 172(1), 381–391 (2004).

38 Horiba M, Martinez LB, Buescher JL *et al.* OTK18, a zinc-finger protein, regulates human immunodeficiency virus type 1 long terminal repeat through two distinct regulatory regions. *J. Gen. Virol.* 88(1), 236–241 (2007).

39 Nishitsuji H, Sawada L, Sugiyama R, Takaku H. ZNF10 inhibits HIV-1 LTR activity through interaction with NF-κB and Sp1 binding motifs. *FEBS Lett.* 589(15), 2019–2025 (2015).

40 Zhu Y, Chen G, Lv F *et al.* Zinc-finger antiviral protein inhibits HIV-1 infection by selectively targeting multiply spliced viral mRNAs for degradation. *Proc. Natl Acad. Sci. USA* 108(38), 15834–15839 (2011).

41 Benjamin R, Banerjee A, Balakrishnan K, Sivangala R, Gaddam S, Banerjee S. Mycobacterial and HIV infections up-regulated human zinc finger protein 134, a novel positive regulator of HIV-1 LTR activity and viral propagation. *PLoS ONE* 9(8), e104908 (2014).

42 Reynolds L, Ullman C, Moore M *et al.* Repression of the HIV-1 5′ LTR promoter and inhibition of HIV-1 replication by using engineered zinc-finger transcription factors. *Proc. Natl Acad. Sci. USA* 100(4), 1615–1620 (2003).

43 Okumura A, Lu G, Pitha-Rowe I, Pitha PM. Innate antiviral response targets HIV-1 release by the induction of ubiquitin-like protein ISG15. *Proc. Natl Acad. Sci. USA* 103(5), 1440–1445 (2006).

44 Lu J, Pan Q, Rong L, Liu S-L, Liang C. The IFITM proteins inhibit HIV-1 infection. *J. Virol.* 85(5), 2126–2137 (2011).

45 Wu H, Sun J, Meng Z, Zhang X, Xu J. HIV-1 infection up-regulating expression of interferon-stimulated gene 15 in cell lines. *Bing du xue bao* 29(5), 480–487 (2013).

46 Zahoor MA, Xue G, Sato H, Murakami T, Takeshima S-N, Aida Y. HIV-1 Vpr induces interferon-stimulated genes in human monocyte-derived macrophages. *PLoS ONE* 9(8), e106418 (2014).

47 Palmer C, Diehn M, Alizadeh AA, Brown PO. Cell-type specific gene expression profiles of leukocytes in human peripheral blood. *BMC Genomics* 7, 115 (2006).

48 Xu K, Geczy CL. IFN-gamma and TNF regulate macrophage expression of the chemotactic S100 protein S100A8. *J. Immunol.* 164(9), 4916–4923 (2000).

49 Hu SP, Harrison C, Xu K, Cornish CJ, Geczy CL. Induction of the chemotactic S100 protein, CP-10, in monocyte/macrophages by lipopolysaccharide. *Blood* 87(9), 3919–3928 (1996).

50 Yen T, Harrison CA, Devery JM *et al.* Induction of the S100 chemotactic protein, CP-10, in murine microvascular endothelial cells by proinflammatory stimuli. *Blood* 90(12), 4812–4821 (1997).

51 Katano M, Okamoto K, Suematsu N *et al.* Increased expression of S100 calcium binding protein A8 in GM-CSF-stimulated neutrophils leads to the increased expressions of IL-8 and IL-16. *Clin. Exp. Rheumatol.* 29(5), 768–775 (2011).

52 Nacken W, Roth J, Sorg C, Kerkhoff C. S100A9/S100A8: myeloid representatives of the S100 protein family as prominent players in innate immunity. *Microsc. Res. Tech.* 60(6), 569–580 (2003).

53 Otsuka K, Terasaki F, Ikemoto M *et al.* Suppression of inflammation in rat autoimmune myocarditis by S100A8/A9 through modulation of the proinflammatory cytokine network. *Eur. J. Heart Fail.* 11(3), 229–237 (2009).

54 Endoh Y, Chung YM, Clark IA, Geczy CL, Hsu K. IL-10-dependent S100A8 gene induction in monocytes/macrophages by double-stranded RNA. *J. Immunol.* 182(4), 2258–2268 (2009).

55 Pechkovsky DV, Zalutskaya OM, Ivanov GI, Misuno NI. Calprotectin (MRP8/14 protein complex) release during mycobacterial infection *in vitro* and *in vivo*. *FEMS Immunol. Med. Microbiol.* 29(1), 27–33 (2000).

56 Schwartz R, Lu Y, Villines D, Sroussi HY. Effect of human immunodeficiency virus infection on S100A8/A9 inhibition of peripheral neutrophils oxidative metabolism. *Biomed. Pharmacother.* 64(8), 572–575 (2010).

57 Muller F, Froland SS, Aukrust P, Fagerhol MK. Elevated serum calprotectin levels in HIV-infected patients: the calprotectin response during ZDV treatment is associated with clinical events. *J. Acquir. Immune Defic. Syndr.* 7(9), 931–939 (1994).

58 Ryckman C, Mccoll SR, Vandal K *et al.* Role of S100A8 and S100A9 in neutrophil recruitment in response to monosodium urate monohydrate crystals in the air-pouch model of acute gouty arthritis. *Arthritis Rheum.* 48(8), 2310–2320 (2003).

59 Hsu K, Passey RJ, Endoh Y *et al.* Regulation of S100A8 by glucocorticoids. *J. Immunol.* 174(4), 2318–2326 (2005).

60 Li Y, Wen B, Chen R, Jiang F, Zhao X, Deng X. Promotion of expression of interferon-stimulated genes in U937 monocytic cells by HIV RNAs, measured using stable isotope labeling with amino acids in cell culture (SILAC). *Arch. Virol.* 160(5), 1249–1258 (2015).

61 Da Conceicao VN, Dyer WB, Gandhi K, Gupta P, Saksena NK. Genome-wide analysis of primary peripheral blood mononuclear cells from HIV + patients-pre-and post- HAART show immune activation and inflammation the main drivers of host gene expression. *Mol. Cell. Ther.* 2, 11 (2014).

62 Zhang X, Bogunovic D, Payelle-Brogard B *et al.* Human intracellular ISG15 prevents interferon-alpha/beta over-amplification and auto-inflammation. *Nature* 517(7532), 89–93 (2015).

- **Deep research on IGS15 that plays an important role on the development of TB-IRIS. The result in our research also supports this.**